

# Using isosbestic points to extract interactions from structure factors

A. A. Louis

Dept. of Chemistry, University of Cambridge, Lensfield Road, CB2 1EW, Cambridge, UK

Inverting scattering experiments to obtain effective interparticle interactions for particles in solution is generally a poorly conditioned problem. More accurate potentials can be obtained through the use of *isosbestic points*, values of  $k$  where the scattering intensity  $I(k)$  or the structure factor  $S(k)$  is invariant to changes in potential well-depth. These points also suggest a new extended corresponding states principle for particles in solution based on the particle density or packing fraction, the second osmotic virial coefficient, and a new measure of potential range.

PACS numbers: 61.20.Gy,82.70Dd

Extracting effective interparticle interactions from experiments is a central objective in chemical physics, because these interactions govern physical behaviour[1]. But like many such inverse problems, this task is complicated. Experimental data is not perfect: statistical fluctuations occur, and results may not be obtainable over a complete parameter range. Moreover, the inversion procedures are often ill conditioned: small differences in the initial input can result in large changes in the final output. This letter concentrates on a well-known class of such problems, namely the inference of (spherically symmetric) effective interparticle pair potentials  $v^{eff}(r)$  from experimental scattering data for particles in solution. For that reason lower effective volume fractions  $\eta$  are investigated than in the better studied case of simple liquids near the triple point, where the dominance of entropic hard-core forces[2] makes it difficult to distinguish between different attractive potentials[2, 3]. Even though at lower volume fractions attractive interactions can determine the structure[4], this letter shows that inversions are equally problematic, albeit for different reasons.

For particles in solution, the scattering intensity  $I(k)$ , measured by light, X-rays, or neutrons, is usually interpreted by dividing  $I(k)$  by the single particle form factor  $P(k)$ , to obtain the structure factor  $S(k) = I(k)/(\rho P(k))$ [5]; here  $\rho = N/V$  is the density. From  $S(k)$ , inferences are then made about the form of the inter-particle interactions  $v^{eff}(r)$ . However, this inversion is ill-conditioned: Within typical experimental accuracy, a single  $S(k)$  at a given state-point can be interpreted with a wide range of different  $v^{eff}(r)$ 's. But, as this letter demonstrates, these problems can be circumvented by introducing a new concept, *isosbestic points* – values of the wave-vector  $k$  for which  $S(k)$  is invariant under changes of the attractive potential well depth. Isosbestic points determine the effective range of the  $v^{eff}(r)$ , and also suggest an extended corresponding states principle for particles in solution, described by three experimentally accessible variables: the range defined by these points, the particle density  $\rho$  and the reduced second osmotic virial coefficient  $B_2^* = B_2/B_2^{HS}$ , where  $B_2^{HS}$  is the second virial coefficient of a hard-sphere (HS) system.

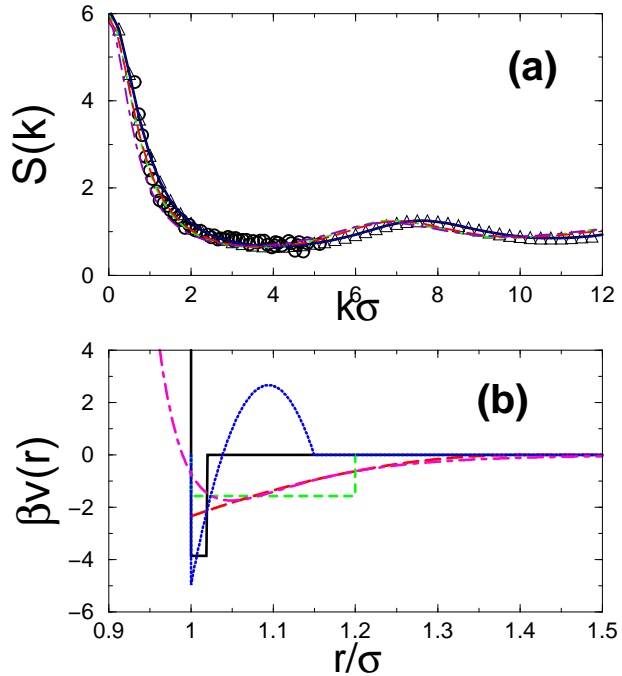


FIG. 1: A single set of experimental data can be interpreted by many different effective potentials. (a) The experimental SANS data (circles) on a microemulsion at packing fraction  $\eta = 0.075$  is from [6]. The open triangles denote the  $S(k)$  from the Baxter model[7] for  $B_2^* = -1.60$ , while the other  $S(k)$  are calculated for the potentials shown in (b). These include SWs with  $\Delta_{SW} = 0.02$  (solid lines) and  $\Delta_{SW} = 0.2$  (dashed), an AO form with  $\Delta_{AO} = 0.4$  (long-dashed), a generalised depletion form with  $\Delta_D = 0.2$  (dotted) and a LJ-12 (dot-dashed) potential. The line-styles in the two graphs correspond with each other.

Fig. 1 helps set the stage and introduce the problem to be addressed here. Experimental data[6], taken from small-angle neutron-scattering (SANS) of a microemulsion composed of small water droplets, coated with a layer of surfactant (AOT), is compared to some theoretical structure factors  $S(k)$ . In the original letter[6] a best fit, using an approximate integral equation technique, yielded a hard-core diameter of  $\sigma = 60\text{\AA}$ , a packing fraction  $\eta = \pi\sigma^3/6 = 0.075$ , and an attractive square well (SW) potential with a range  $\Delta_{SW} = 0.02\sigma$  and a

well depth of  $\beta v(\sigma) = 3.85$ . The quality of the integral equation fit was then confirmed by independent computer simulations. However, as strikingly demonstrated by Fig. 1, a wide range of other potentials, depicted in Fig. 1(b), also lead to fits of similar accuracy. These include HSSs with attractive SWs of two different ranges  $\Delta_{SW}$ , an Asakura-Oosawa (AO) depletion potential[8] of range  $\Delta_{AO}$ , an alternate simplified depletion potential of range  $\Delta_D$  showing the effects of solvation layers[9], as well as a Lennard-Jones-n (LJ-n) potential, defined as:

$$v(r) = 4\epsilon \left( \left( \frac{\sigma}{r} \right)^{2n} - \left( \frac{\sigma}{r} \right)^n \right), \quad (1)$$

with  $n = 12$ . The  $S(k)$  are calculated within the Percus Yevick (PY) integral equation closure[2, 10], and are close to the analytical PY solution of Baxter's model[7].

Improving significantly on these pioneering experiments is hard.  $S(k)$  is obtained by dividing  $I(k)$  through by  $P(k)$ , which is only approximately determined, and which rapidly decays to zero for increasing  $k\sigma$ , so that achieving better accuracies for a larger  $k\sigma$  range is very difficult. Moreover, there are few alternative methods to directly measure the interparticle interactions. In contrast, for simpler atomic or molecular systems, gas-phase experiments or ab-initio calculations can provide accurate independent estimates of the interactions, and impose important constraints on the potential forms with which to fit the experimental data[11]. Although increasingly accurate techniques being developed for the real-space measurement of the  $v^{eff}(r)$  of particles in solution[12], these are often limited to certain particle types or sizes.

The upshot of Fig. 1 is that deducing an effective potential from experimental scattering data at one state point is difficult; *the inversion is ill-conditioned*. Clearly more information is needed to interpret the data[13].

But first, what can be inferred from a single  $S(k)$ ? One hint comes the Baxter model, which is completely determined by the packing fraction  $\eta$  and the reduced osmotic virial coefficient  $B_2^*$  or equivalently, the Baxter parameter, defined as  $\tau = \frac{1}{4}/(1 - B_2^*)$ . The  $S(k)$  in Fig. 1, with effective  $\tau$  parameters ranging from  $\tau = 0.093$  to  $\tau = 0.10$  are all close to the Baxter model result with  $\tau = 0.096$ . To first order therefore, measuring a single  $S(k)$  in this regime of low packing fraction, commonly encountered for particles in solution, does not result in much more information about the effective potential than the reduced second virial coefficient  $B_2^*$ . Just as in simple liquids inversions are hard because the  $S(k)$  resemble those of HSSs[2], here difficulties arise because they are close to the Baxter  $S(k)$ .

To make further progress, measurements at other state points are necessary. This is done in Figs. 2(a)-(d), which depict the  $S(k)$  calculated for four LJ-n potentials at different temperatures. A best fit to the Baxter model  $S(k)$  at each temperature would result in  $B_2^*$  as a function of

temperature. But there is clearly more information in these curves: Each of the four  $v^{eff}(r)$  results in a different set of *isosbestic points*, where the  $S(k)$  is invariant for different temperatures. Fig. 2(e) shows that the first isosbestic point  $k_1\sigma$  increases with increasing  $n$ , reflecting the decrease of the range of the LJ-n potential (1) depicted in Fig. 2(f). (Error bars in Fig 2(e) reflect the approximate nature of the isosbestic points.)

These observations can be quite easily rationalised by the following simple theory: If the total correlation function  $h(r) = g(r) - 1$  is split into two parts, with  $h_0(r) = -1$  for  $r < \sigma$ , and  $h_1(r) = g(r) - 1$  for  $r \geq \sigma$ , then the structure factor  $S(k) = 1 + \rho\hat{h}(k)$  simplifies to

$$S(k) = 1 + \frac{4\pi\rho}{k} j_1(k) + \rho\hat{h}_1(k), \quad (2)$$

where  $j_1(k)$  is the first spherical Bessel function, and  $\hat{h}_1(k)$  is the Fourier Transform (FT) of  $h_1(r)$ . For potentials with a hard-core, such as most of those depicted in Fig. 1(b), this is exact, but even for the LJ-n potentials this is a good approximation[14]. Since  $\hat{h}_0(k) = \frac{4\pi\rho}{k} j_1(k)$  is independent of temperature (barring small effective  $\sigma$  effects), Eq. 2 suggests that isosbestic points occur whenever  $\hat{h}_1(k) = 0$ .

It has already been pointed out that in many experimentally relevant cases with low  $\eta$ , the  $g(r)$  are surprisingly well approximated by a simple form  $g(r) = \exp(-\beta v(r))$ [4, 15], as explicitly demonstrated in Fig. 3. This simple approximation, equivalent to taking a Mayer function[2] for  $h(r)$ , works best for particles with short range attractive potentials. These can become quite deep, leading to large values of  $g(r)$  near contact, well before the system crosses a liquid-liquid or liquid-solid phase-line. Within this approximation, the dominant effect of varying the temperature is to change the amplitude of  $h_1(r)$  (as demonstrated in Fig. 3(b)). To first order, the period of  $\hat{h}_1(k)$  is not affected and each  $k\sigma$  where  $\hat{h}_1(k) = 0$  leads to an isosbestic point. For an infinitely narrow potential, the isosbestic points would be at  $k_n\sigma = n\pi$ , but for a finite potential range there is a phase-shift, which explains why the  $k_n\sigma$  move progressively further from  $n\pi$  with increasing range. The excellent accuracy of this simple Mayer function theory for the first isosbestic point  $k_1\sigma$  is demonstrated by the solid line in Fig. 2(e).

The examples depicted in Fig. 2 are at a relatively low packing fraction, but the isosbestic points are robust up to packing fractions of at least  $\eta = 0.2$ , as shown in Fig. 4(a)[16]. These points are accurately described by the simple theory, described above.

If varying a parameter leads to isosbestic points, then this suggests that the well-depth of  $v^{eff}(r)$  is changing while the range is not. When combined with the variation of  $B_2$ , this can help fix the form of  $v^{eff}(r)$ . However, this information may still not be sufficient, since

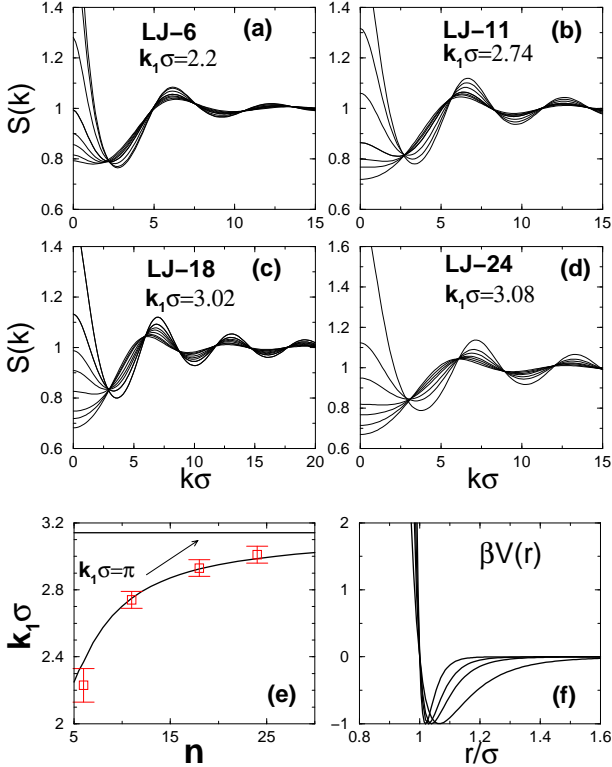


FIG. 2: (a)-(d)  $S(k)$  were calculated at  $\eta = 0.0576$  and at different temperatures for each of the four LJ-n potentials  $v^{eff}(r)$  given by Eq. (1). Different  $v^{eff}(r)$  lead to different isosbestic points  $k_1\sigma$ . (e) The first isosbestic point  $k_1\sigma$  approaches  $\pi$  with increasing  $n$ . A simple theory (solid line), described in the text, fits the data well. (f) The range of the LJ-n potentials in (a)-(d) decreases with increasing  $n$ .

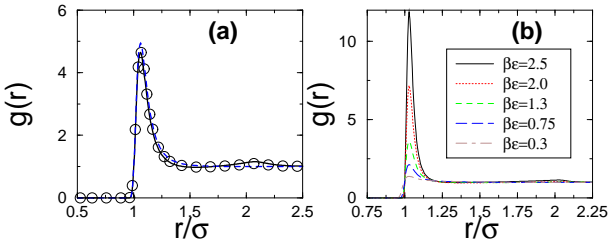


FIG. 3: (a) The PY approximation (solid line) very accurately reproduces these molecular dynamics simulations[10] of a LJ-12 potential at  $\beta\epsilon = 1.6$ , and  $\eta = 0.1$ . The simpler  $g(r) = \exp(-\beta v(r))$  form (dashed lines) is also accurate. (b) When the temperature is changed, the dominant effect on  $g(r)$ , calculated here with PY, is to change its amplitude.

the well-depth of  $v^{eff}(r)$  may depend in an (unknown) non-linear fashion on the parameters like the temperature  $T$ , the pH, and salt or other additive concentration. Furthermore, as shown in Fig. 4(b), different potential shapes, picked to have the same isosbestic points, can generate similar  $S(k)$  for each value of  $B_2^*$ .

This similarity of the  $S(k)$  ties in with the work of Noro and Frenkel (NF), who proposed that many prop-

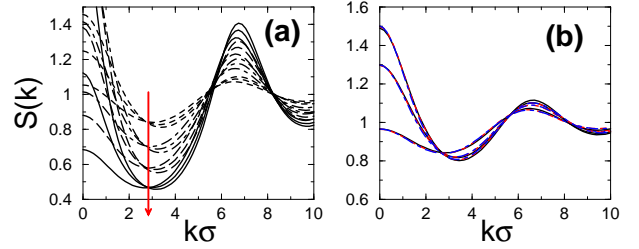


FIG. 4: Fig (a) The position of isosbestic points barely varies with density for LJ-12, shown here for three temperatures  $\beta\epsilon = 1.5, 1.33, 1.09$  at each density  $\eta = 0.05, 0.1, 0.15, 0.2$ . The line with the arrow denotes  $k_1\sigma$  for increasing  $\eta$ . (b) Three potentials leading to the same isosbestic points: SW ( $\Delta_{SW} = 0.26$ ) (solid lines), AO ( $\Delta_{AO} = 0.6$ ) (dashed lines) and LJ-22 (dot-dashed lines) for  $\eta = 0.05$  and  $B_2^* = 0, -0.719, -1$  (plots in descending order of  $B_2$  at  $k = 0$ ).

erties of particles in solution could be understood from an extended corresponding state principle based on the variables  $\eta$ ,  $B_2^*$ , and an effective well depth  $\beta\epsilon$ [17]. However, the three potentials shown in Fig. 4(b) do not have the same well-depth, while still showing similar  $S(k)$ . This suggests an alternative corresponding states principle based on the variables  $\eta$ ,  $B_2^*$ , and an effective range  $\Delta_{eff}$  related to the isosbestic points. In fact, as NF point out, the potential range is not always uniquely defined when comparing different  $v^{eff}(r)$ 's. They suggested a non-linear mapping based on  $B_2^*$  to derive an effective SW range for each potential they consider. I used a simpler linear mapping to define the range  $\Delta_{eff}$  of a given potential as identical to that of a SW with the same  $k_1\sigma$ . For the LJ-n potentials this criterion reduces to the distance  $r - \sigma$  where  $\beta v(r)$  reaches  $1/4$  of its maximum depth, for the AO potential the effective SW range is  $\Delta_{eff} \simeq 0.42\Delta_{AO}$ , and for the hardcore Yukawa potential, with an attractive tail of the form  $v(r) = \epsilon \exp(-r/\lambda)$  for  $r > \sigma$ , the mapping is  $\Delta_{eff} \simeq 1.15\lambda$ . The results are depicted in Fig. 5, and show that these simple linear mappings successfully define an effective range for each potential type. An accurate approximation of  $k_1\sigma$  for the (effective) SW is given by  $k_1\sigma \approx \pi/(1 + \Delta_{eff}/2 + \Delta_{eff}^2/12)$ , which follows from an expansion of the exact solution to the simple theory of isosbestic points.

Another argument for including the  $\Delta_{eff}$  (instead of the well-depth) as one of the relevant 3 variables is that the range determines the topology of the phase-diagram[17]. The critical range below which the fluid-fluid transition becomes metastable to the fluid-solid line is at  $\Delta_{eff} \approx 0.15$  for all four potentials (SW, AO, Yukawa and LJ-n), something consistent with what NF found. In addition,  $\Delta_{eff}$  is directly experimentally accessible through  $k_1\sigma$ . For example, taking advantage of the proximity of a metastable fluid-fluid critical point to enhance nucleation, a proposal recently made for protein solutions[18], would involve tailoring solution con-

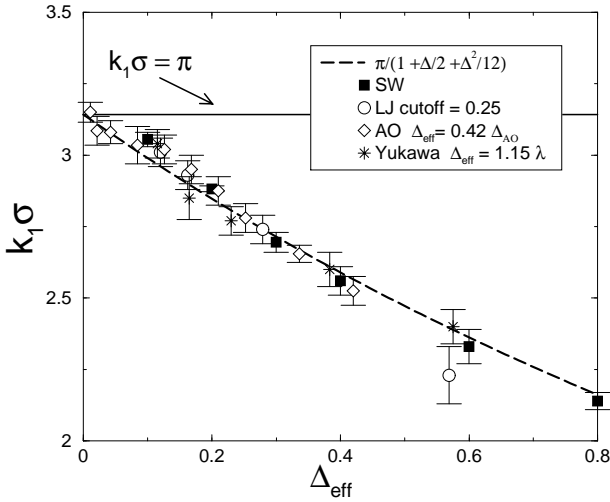


FIG. 5: Defining effective range parameters from isosbestic points. For each potential type a simple linear mapping to an effective square well range  $\Delta_{eff}$  was used (as described in the text). The long-dashed line denotes an accurate analytical approximation for the isosbestic points of square-well fluids which can be used to estimate the  $\Delta_{eff}$  for different potentials directly from the  $k_1\sigma$ .

ditions such that the measured isosbestic point is just above  $k_1\sigma = 2.92$ , so that  $\Delta_{eff}$  is just below 0.15.

In summary then, extracting effective potentials  $v^{eff}(r)$  from  $S(k)$  at the lower packing fractions typically encountered for particles in solution is a poorly conditioned problem. Whereas in simple liquids the HS model describes the dominant features of the  $S(k)$ , here the Baxter model appears to be the fundamental underlying model for  $S(k)$  around which different attractive potentials only induce a mild perturbation. More information can be obtained by studying the isosbestic points, which help determine the range  $\Delta_{eff}$  of the potentials. Together with  $\eta$  and  $B_2^*$ ,  $\Delta_{eff}$  can be used to define an extended corresponding states principle. Particles in solution with similar values of these three parameters should have similar properties, such as the relative stability of the fluid-fluid and fluid-solid binodals. In other words, many solution properties could be deduced without having to actually invert to an explicit form of  $v^{eff}(r)$ .

Another advantage of a description based on these variables is that they are directly experimentally accessible. In fact, numerous examples of isosbestic points can be found in the literature, ranging from colloids with short-range sticky coats[19], to colloid-polymer mixtures[20], to globular proteins[21], to magnetic colloids[22] and to colloid-micelle mixtures[23]. Interestingly, these points should also appear in  $I(k)$ , although determining  $\Delta_{eff}$  still depends on an accurate  $P(k)$ . Future work will consider the role of size polydispersity (expected to mainly affect higher order  $k_n\sigma$ ) and the existence of isosbestic points for non-spherical objects.

The author thanks P. Bartlett for first bringing isos-

bestic points to his attention, J. P. K. Doye for helpful discussions, and The Royal Society for financial support.

- [1] W.G. McMillan and J.E. Mayer, *J. Chem. Phys.* **13**, 276 (1945); C.N. Likos, *Phys. Rep.* **348**, 267 (2001).
- [2] J.P. Hansen and I.R. McDonald, *Theory of Simple Liquids*, 2nd Ed. (Academic Press, London, 1986).
- [3] L. Reatto, *Phil. Mag. A* **58**, 37 (1986); L. Reatto, D. Levesque, and J.J. Weis, *Phys. Rev. A* **33**, 3451 (1986).
- [4] A.A. Louis, *Phil. Trans. Roy. Soc. A* **359**, 939 (2001).
- [5] R. J. Hunter, *Foundations of Colloid Science*, 2nd Ed. (Oxford University Press, Oxford 2001).
- [6] J.S. Huang, S.A. Safran, M.W. Kim, G.S. Grest, M. Kotlarchyk, and N. Quirk, *Phys. Rev. Lett.* **53**, 592 (1984).
- [7] R.J. Baxter, *J. Chem. Phys.* **49**, 2770 (1968).
- [8] S. Asakura and F. Oosawa, *J. Polym. Sci., Polym. Symp.* **33**, 183 (1958), A. Vrij, *Pure Appl. Chem.* **48**, 471 (1976).
- [9] B. Götzelmann, R. Evans, and S. Dietrich, *Phys. Rev. E* **57**, 6785 (1998)
- [10] More sophisticated closures[2] could be used, but for the low  $\eta$  regime discussed here, the PY approximation is adequate. This is demonstrated in Fig. 3, where the  $g(r)$  from a molecular dynamics simulation, performed with the MOLDY code (K. Refson, *Comput. Phys. Commun.* **126**, 310 (2000)) on a box of 1024 atoms, is virtually indistinguishable from the PY result. Similar accuracy was found for other potentials and parameters, and confirms the findings of other authors (See e.g. K. Shukla and R. Rajagopalan, *Mol. Phys.* **81**, 1093 (1994); M. Dijkstra, J. Brader, and R. Evans *J. Phys.: Condens. Matter* **11**, 10079 (1999) and references therein.). Another reason I use the PY closure is to facilitate comparisons with the Baxter model[7], which is only solved within PY.
- [11] G. C. Maitland *et al.*, *Intermolecular Forces: Their Origin and Determination*, (Clarendon Press, Oxford, 1987).
- [12] See e.g. J.N. Israelachvili, *Intermolecular and Surface Forces* (Academic Press, London, 1992), R. Verma *et al.* *Phys. Rev. Lett.* **81**, 4004 (1998); C. Bechinger *et al.*, *ibid* **83**, 3960 (1999).
- [13] I should add that this is not an implicit critique of ref[6], where other physical considerations were indeed used to infer the suggested short ranged potential.
- [14] There are several similar ways to define an effective  $\sigma_{eff}$  for a LJ- $n$  potential, see e.g.[2]. A more careful analysis shows that for our examples, these don't differ much from  $\sigma$ , and have a marginal effect on the isosbestic points.
- [15] A.A. Louis, *Phys. Rev. Lett.* **84**, 1840 (2000).
- [16] The isosbestic points typically move to a marginally higher  $q$  with increasing  $\eta$ , an effect also seen for the Baxter model; this can be used for a small correction to isosbestic points. (A.A. Louis, unpublished).
- [17] M.G. Noro and D. Frenkel, *J. Chem. Phys.* **113**, 2941 (2000) (and references therein).
- [18] P.R. ten Wolde and D. Frenkel, *Science* **277**, 1973 (1997).
- [19] M. H. G. Duits, R. P. May, A. Vrij, and C. G. de Kruif, *Langmuir* **7**, 62 (1991).
- [20] X. Ye, T. Narayanan, P. Tong, and J.S. Huang, *Phys. Rev. Lett.* **76**, 4640 (1996).
- [21] A. Tardieu *et al.* *J. Crystal Growth* **196**, 193 (1999).
- [22] E. Dubois, V. Cabuil, F. Boué, and R. Perzynski, *J. Chem. Phys.* **111**, 7147 (1999).
- [23] P. Bartlett, (unpublished)